Luminosity determination for the deutron-deutron reactions using free and quasi-free reactions with WASA-at-COSY detector

M. Skurzok[a], W. Krzemien[a,b] and P. Moskal[a,c] for the WASA-at-COSY collaboration

In November 2010 the search for the ^{4}He-η bound state was performed by measuring the excitation functions for $dd \to {}^3\mathrm{He}n\pi^0$ and $dd \to {}^3\mathrm{He}p\pi^-$ reactions near the η production threshold. The measurement was carried out with a deuteron beam momentum ramping from 2.127 GeV/c to 2.422 GeV/c, corresponding to the range of the excess energy Q∈(-70,30) MeV. During an acceleration process the luminosity could vary due to beam losses caused by the interaction with the target and with the rest gas in the accelerator beam line, as well as due to the changes in the beam-target overlap correlated with momentum variation and adiabatic shrinking of the beamsize. Therefore, it was necessary to determine not only the total integrated luminosity but also its dependence on the excess energy. The total integrated luminosity is determined based on the $dd \to {}^3\mathrm{He}n$ and quasi free $pp \to pp$ reactions for which the cross sections were already experimentally established. Because of the acceptance variation for the beam momentum range for which ^{3}He ions are stopped between FRH3 and FRH4, the excess energy dependence of the luminosity is determined based on quasi-free $pp \to pp$ reaction for which the WASA acceptance is a smooth function of the beam momentum.

Independent analyses for the $dd \to {}^3\mathrm{He}n$ and quasi free $pp \to pp$ reactions were carried out. In case of the first, binary reaction, the low-energetic ^{3}He ions were stopped in the 3rd layer of the Forward Range Hodoscope, while high-energetic ions were stopped in the 4th layer. The helium identification was based on the ΔE-ΔE method. The outgoing neutrons were identified using the missing mass technique. In order to reduce background originating from quasi-free $dp(n) \to{}^3 \mathrm{He}n\pi^0$, the cut in missing mass m_x vs. missing energy E_x spectrum was applied as it is presented in upper panel of Fig. 1. Additionally, for high beam momentum region background was subtracted via fitting the signal and background function to the missing mass spectrum for different intervals of $cos\theta^*$ and beam momentum, what is presented in the lower panel of Fig. 1.

In order to calculate the total integrated luminosity, the number of events, efficiency, as well as cross section was determined for 5 intervals of $cos\theta^*$ in the range from 0.88 to 0.98 and 5 intervals of excess energy Q in the range from -70 MeV to 30 MeV corresponding to the angular range of the reaction and the beam momentum ramping, respectively. The integrated luminosity was then calculated for each (i,j)-th interval in following way:

$$L_{i,j}^{int} = \frac{N_{i,j}}{\epsilon_{i,j} \cdot \frac{d\sigma_{i,j}}{d(cos\theta^*)} \cdot \Delta(cos\theta^*)}, \qquad (1)$$

where $\frac{d\sigma_{i,j}}{d(cos\theta^*)}$ is the cross section determined based on parametrization of SATURNE data [1] described in details in Ref. [2] corrected in our angular region of interest [3], while $\Delta(cos\theta^*)$ is the width of the $cos\theta^*$ interval and $\epsilon_{i,j}$ is overall efficiency including reconstruction ef-
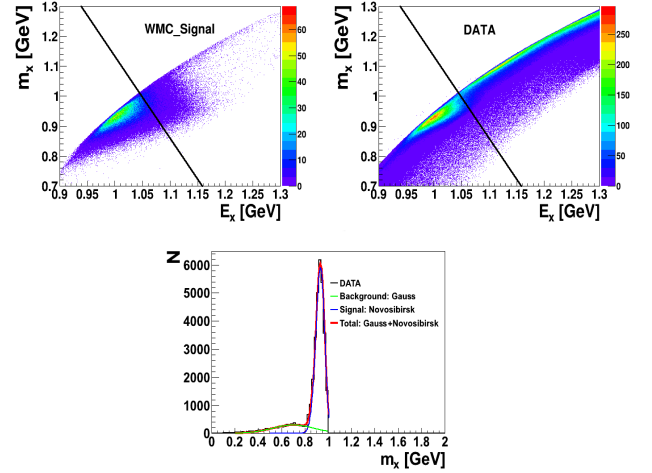
Fig. 1: (upper panel) The missing mass m_x vs. missing energy E_x spectrum for simulations (left) and DATA (right). Applied cut is marked with black line. (lower panel) The missing mass m_x spectrum for i. e. $cos\theta^*$ ∈(0.96,0.98) and Q∈(0,5) MeV. The red line shows fit to the signal and background while green line shows fit of the Gauss function to the background. Signal peak is marked as a blue line.

ficiency and geometrical acceptance of the detector determined based on the Monte Carlo simulations.

The preliminary luminosity dependence of $cos\theta^*$ for whole excess energy range is presented in Fig. 2. The total integrated luminosity was calculated as a weighted average of the luminosities determined for individual $cos\theta^*$ intervals:

$$L_{dd\to{}^3Hen}^{tot} = \frac{\sum_{i=1}^5 L_i \frac{1}{(\Delta L_i)^2}}{\sum_{i=1}^5 \frac{1}{(\Delta L_i)^2}}, \qquad (2)$$
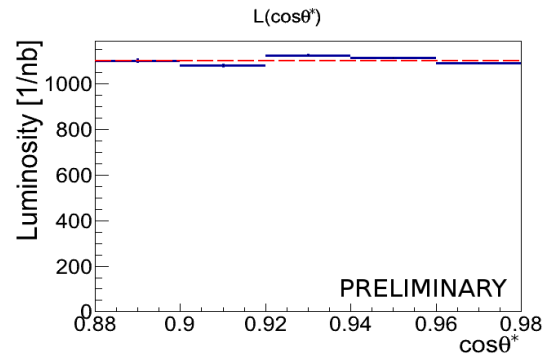
Fig. 2: Integrated luminosity as a function of $cos\theta^*$. The statistical uncertainties are marked as a vertical bars. The preliminary established weighted average of integrated luminosity is marked as a dashed red line. The analysis was carried out with condition that the number of "neutral clusters" reconstructed in the Central Detector is less than 2.

The average integrated luminosity with its statistical uncertainty equals $L_{dd \to ^3Hen}^{tot} = (1102 \pm 2) nb^{-1}$ and is marked in Fig. 2 with dashed red line.

In order to determine the luminosity dependence on the beam momentum we used the quasi-elastic proton-proton scattering in the deuteron-deuteron collisions: $dd \to ppn_{sp}n_{sp}$. In this reaction protons from the deuteron beam are scattered on the protons in the deuteron target. We assume that the neutrons are acting only as spectators which means that they do not take part in reactions but move with the Fermi momentum of their parent deuterons. In the case of quasi-free proton-proton scattering the formula for the calculation of the integrated luminosity can be written in the following form [4]:

$$L = \frac{N_0 N_{exp}}{2\pi I} \quad (3)$$

where $I = \int_{\Delta\Omega(\theta_{lab},\phi_{lab})} \frac{d\sigma}{d\Omega}(\theta^*, \phi^*, p_{F_{1,2}}, \theta_{F_{1,2}}, \phi_{F_{1,2}}) \times f(p_{F_{1,2}}, \theta_{F_{1,2}}, \phi_{F_{1,2}}) dp_{F_{1,2}} dcos\theta_{F_{1,2}} d\phi_{F_{1,2}}, d\phi^* dcos\theta^*.$

The formula is determined based on the fact, that the number of quasi-free scattered protons into the solid angle $\Delta\Omega(\theta_{lab},\phi_{lab})$ is proportional to the integrated luminosity L, as well as to the inner product of the differential cross section for scattering into the solid angle around θ^* and ϕ^* angles expressed in proton-proton CM system: $\frac{d\sigma}{d\Omega}(\theta^*, \phi^*, p_{F_{1,2}}, \theta_{F_{1,2}}, \phi_{F_{1,2}})$ and the probability density of the Fermi momentum distributions: $f(p_{F_{1,2}}, \theta_{F_{1,2}}, \phi_{F_{1,2}})$ inside the deuteron beam and deuteron target, respectively. The detailed description of the luminosity calculation for quasi-free reaction can be found in Ref. [3, 4]. Due to the complex detection geometry, a solid angle corresponding to a particular part of the detector cannot be, in general, expressed in a closed analytical form. Therefore, the integral in above equation was computed with the Monte Carlo simulation programme, containing the geometry of WASA detection system and taking into account detection and reconstruction efficiencies. For each of N_0 simulated event we assign a weight corresponding to the differential cross section, which is uniquely determined by the scattering angle and the total proton-proton collision energy $\sqrt{s_{pp}}$. The cross sections were calculated used the cross section values for proton-proton elastic scattering $pp \to pp$ computed based on the SAID program [5] because the EDDA collaboration data base [6] does not cover the whole interesting energy region. The distribution of the effective beam momentum as well as a comparison of the SAID calculations and the existing differential cross section from the EDDA measurements are shown in Fig. 3. As we can see, the differential cross sections calculated using the SAID programme are in agreement with distributions measured by the EDDA collaboration. The differential cross section for appropriate p_{beam}^{prot} and θ^* was calculated using bilinear interpolation in the momentum-scattering angle plane.

The number of experimental events N_{exp} was determined based on conditions and cuts described in details in reference [7]. In the analysis, at the beginning, we carried out primary events selection applying condition of exactly one charged particle in the Forward Detector
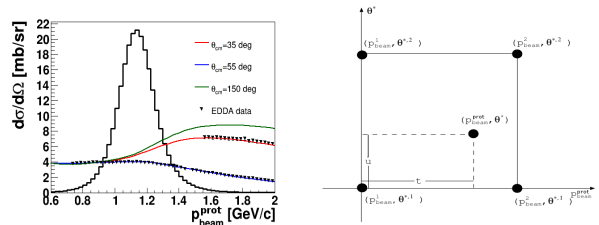
Fig. 3: (left) Differential cross sections for proton-proton elastic scattering as a function of the beam momentum for a three values of the scattering angle θ^* in the CM frame. Black points show EDDA collaboration data [6], while lines denote SAID calculations [5]. Distribution of the effective beam momentum for quasi-free $pp \to pp$ reaction calculated for the deuteron beam momentum range $p_{beam} \in (2.127, 2.422) GeV/c$ is also presented in the figure. (right) Bilinear interpolation of the differential cross section $\frac{d\sigma}{d\Omega}(p_{beam}^{prot}, \theta^*)$. The figure is adopted from [4].

(FD) and one particle in the Central Detector (CD). In Ref. [7] we can find detailed studies of the possible background reaction contributions. In case of this analysis the dominating background processes are $dd \to ppn_{sp}n_{sp} \to d\pi^+n_{sp}n_{sp}$, $dd \to d_b p_t n_{sp}$ and $dd \to pp_{sp}nn_{sp}$, where the subscripts sp, b and t denote the spectators, particles from the beam and from the target, respectively. In order to reject the events corresponding to the charged pions registered in the Central Detector, the cut on the energy deposited in the Electromagnetic Calorimeter (Cal) vs. energy deposited in Plastic Scintillator Barrel (PSB) spectrum was applied and is presented in the upper panel of Fig. 4.
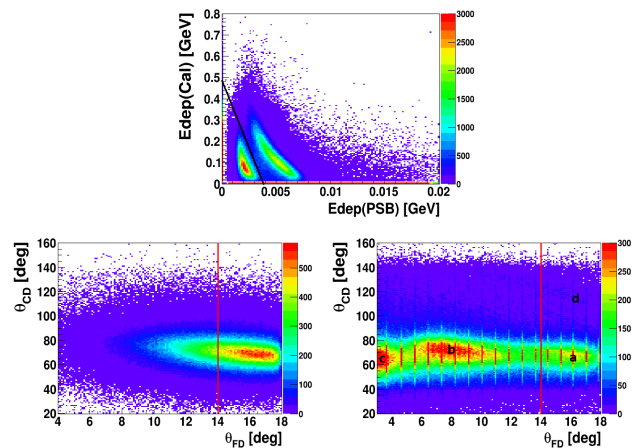
Fig. 4: (upper panel) Experimental spectrum of the energy loss in the Plastic Scintillator Barrel shown as a function of the energy deposited in the Electromagnetic Calorimeter. The applied cut is shown as a black line. Pions in data spectrum are concentrated for Edep(PSB) around 0.003GeV. (lower panel) Correlations between the polar angles θ_{FD} and θ_{CD} for the WMC Simulations of $dd \to ppn_{sp}n_{sp}$ reaction (left) and obtained in experiment (right). Applied cut is marked with red line. The indicated area correspond to the: a) $dd \to ppn_{sp}n_{sp}$, b) $dd \to d_b p_t n_{sp}$ and $dd \to ppn_{sp}n_{sp}$, c) $dd \to pp_{sp}nn_{sp}$, d) $dd \to p_b d_t n_{sp}$.

In order to separate quasi-elastic p-p scattering from the quasi-elastic d-p scattering the cut in polar angle θ_{FD} was applied and is shown in lower panel of Fig. 4. In order to subtract the background coming from $dd \rightarrow p_b d_t n_{sp}$ reaction, the range $\theta_{CD} \in (40,100)°$ was taken into account in further analysis. Additionally, the background was subtracted in $\Delta\phi = \phi_{FD} - \phi_{CD}$ spectrum. In order to symetrize the background instead of $|\Delta\phi|$ we define $(2\pi + \Delta\phi)\mathrm{mod}2\pi$. Afterwards, the background was fitted with 1st order polynomial for each of excess energy Q intervals. The exemplary $(2\pi + \Delta\phi)\mathrm{mod}2\pi$ spectrum is presented in Fig. 5.
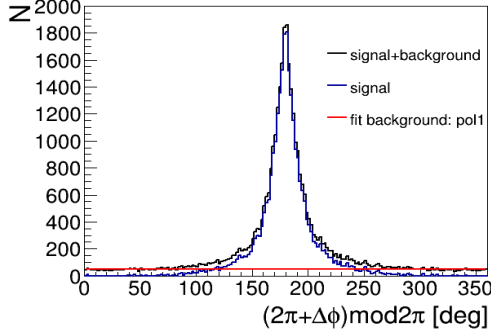
Fig. 5: Distributions of $(2\pi + \Delta\phi)\mathrm{mod}2\pi$, where $\Delta\phi = \phi_{CD} - \phi_{FD}$ is the difference of azimuthal angles in Central Detector and Forward Detector. The example spectrum for one of the Q intervals (black line) with marked fit function (red line) and signal peak after background subtraction (blue line) is presented.

After all cuts and conditions described above, the number of experimental data was determined and the luminosity was calculated for each excess energy interval taking into account also prescaling factor of the applied experimental trigger equal to 4000 as well as shadowing effect equal to 9% [3]. The preliminary result is presented in Fig. 6. The statistical uncertainty of each point is about 1%. The luminosity variation (increase in the excess energy range from about -70MeV to -40MeV, and then decrease) is caused by the change of the beam-target overlapping during the acceleration cycle and also by adiabatic beam size shrinking [8]. The obtained total integrated luminosity within its statistical uncertainty is equal to $L^{tot}_{dd \rightarrow ppn_{sp}n_{sp}} = (1329 \pm 2)nb^{-1}$. For further analysis the luminosity was fitted by third order polynomial $aQ^3 + bQ^2 + cQ + d$. The fitted function is marked with the red line in Fig. 6.

To sum up, the total integrated luminosity calculated based on $dd \rightarrow {}^3\mathrm{He}n$ and the quasi-free $dd \rightarrow ppn_{sp}n_{sp}$ reactions with statistical, systematical and normalization error are equal to $L^{tot}_{dd \rightarrow {}^3\mathrm{He}n} = (1102 \pm 2_{stat} \pm 28_{syst} \pm 107_{norm})nb^{-1}$ and $L^{tot}_{dd \rightarrow ppn_{sp}n_{sp}} = (1329 \pm 2_{stat} \pm 108_{syst} \pm 64_{norm})nb^{-1}$, respectively. The systematical and normalization errors were calculated by adding in quadrature the appropriate contributions described in details in Ref. [3].
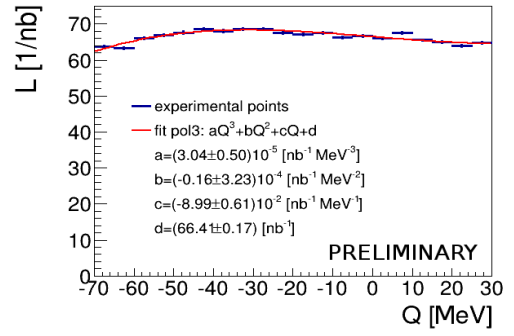
Fig. 6: Integrated luminosity calculated for experimental data for quasi-free $dd \rightarrow ppn_{sp}n_{sp}$ reaction (blue points) with fitted third order polynomial function (red line).

References:

[1] G. Bizard et al., *Phys. Rev.* **C22**, 1632 (1980).
[2] A. Pricking, *PhD Thesis*, Tuebingen University, Germany (2010).
[3] M. Skurzok, W. Krzemien, P. Moskal, *Acta. Phys. Pol.* **B46**, 133 (2015).
[4] P. Moskal and R. Czyżykiewicz, *AIP Conf. Proc.* **950**, 118 (2007).
[5] The CNS Data Analysis Center, http://www.gwu.edu.
[6] D. Albers et al., *Phys. Rev. Lett.* **78**, 1652 (1997).
[7] W. Krzemień, *PhD Thesis, Jagiellonian University, arXiv:nucl-ex/1202.5794* (2011).
[8] B. Lorentz - *private communication* (2014).

[a] M. Smoluchowski Institute of Physics, Jagiellonian University, 30-059 Cracow, Poland

[b] National Centre for Nuclear Research, 05-400 Otwock-Świerk, Poland,

[c] Institut für Kernphysik, Forschungszentrum Jülich, Germany.